Catena 133 (2015) 403–411

Contents lists available at ScienceDirect

Catena

journal homepage: www.elsevier.com/locate/catena

Effects of vegetation and physicochemical properties on solute transport in reclaimed soil at an opencast coal mine site on the Loess Plateau, China

Qing Zhen [a,c], Wenmei Ma [b], Mingming Li [e], Honghua He [a,b], Xingchang Zhang [a,b,*], Yi Wang [d]

[a] State Key Laboratory of Soil Erosion and Dryland Farming on Loess Plateau, Institute of Soil and Water Conservation, Chinese Academy of Sciences and Ministry of Water Resources, Yangling, Shaanxi 712100, China
[b] Institute of Soil and Water Conservation, Northwest A&F University, Yangling, Shaanxi 712100, China
[c] University of Chinese Academy of Sciences, Beijing 100049, China
[d] State key Laboratory of Loess and Quaternary, Institute of Earth Environment, Chinese Academy of Sciences, Xi'an 710075, China
[e] College of Environment and Planning, Henan University, Kaifeng, Henan 475001, China

ARTICLE INFO

Article history:
Received 17 September 2014
Received in revised form 21 April 2015
Accepted 12 June 2015
Available online 24 June 2015

Keywords:
Reclaimed soil
Soil properties
Solute transport
BTC
Vegetation

ABSTRACT

Mine soils are often polluted and degraded. The objectives of this study were to assess the effects of soil properties and vegetation on soil solute transport in reclaimed soil at an opencast coal mine site on the Loess Plateau. Four reclaimed areas with different vegetation types were selected for the analysis of physical and chemical properties. The miscible displacement technique was used to obtain the breakthrough curves (BTCs) of NO_3^- ion transport in undisturbed soil columns, which were taken from the soil profiles of the different sites. The chemical properties, such as total N, P, K and SOM, exhibited low contents, and the soil physicochemical properties showed high heterogeneity between different depths and different reclaimed areas. The structural stability index was less than 5%. The initial and entire penetration times were longer in the deeper layers than in the top layer. The BTCs of NO_3^- were fitted well by the deterministic equilibrium convection dispersion equation (CDE) model. Preferential flow and transport were found in the soil columns. The reclaimed soil had poor structure, and planting vegetation improved the physiochemical properties of the soil. The soil solute transport parameters exhibited high heterogeneity between different samples and were significantly correlated with soil bulk density and soil texture, which were highly influenced by vegetation and human activities. In the process of land reclamation, increasing the bulk density and selecting fine-textured soils could reduce the average soil pore water velocity and the dispersivity coefficient, thereby extending the solute penetration time.

1. Introduction

Coal plays a leading role in the energy structure of China and contributes greatly to China's economic development (Wang et al., 2006). However, coal mining activities, especially opencast mining, have caused serious damage to the environment, including the elimination of vegetation, permanent topographic changes, dramatic changes in the soil and subsurface geological structure and disruption of the surface and subsurface hydrologic regimes (Keskin and Makineci, 2009). Coal mining produces a large amount of stripped soils, coal gangue, tailings and other solid wastes, which are buried or deposited in piles, replacing a large area of arable land with bare ground. Mine soils are usually degraded and are characterized by poor soil structure, high bulk density, low pH, low nutrient availability, low water holding capacity, low structural stability and low biomass productivity (Asensio et al., 2013; Palumbo et al., 2004; Shrestha and Lal, 2006). Reclamation of these bare ground soils is necessary to minimize the risk of land degradation (Pedrol et al., 2010).

Chemical, physical and biological properties are always selected as the main soil quality indicators and are monitored over time to determine changes in soil quality, i.e., improving, degrading, or stable (Carter et al., 1997; Shukla et al., 2004a). Several authors have studied the degradation and reclamation of mined soils and suggest that the establishment of vegetative cover should be encouraged. The selection of appropriate vegetation and soil amendments is essential to stabilizing a bare area and remediating adverse physical and chemical properties (Asensio et al., 2013; Keskin and Makineci, 2009; Wong, 2003; Zhao et al., 2013). Shukla et al. (2004a) found that bulk density was the most discriminating factor and that water-stable aggregation was the most commonly measured soil attribute and the most dynamic soil quality indicator for reclaimed mine soils in southeastern Ohio. The authors also found that there were no significant differences in several soil properties, such as bulk density and SOC content, between undisturbed (unmined) soil

* Corresponding author.
E-mail address: zhangxc@ms.iswc.ac.cn (X. Zhang).

http://dx.doi.org/10.1016/j.catena.2015.06.009
0341-8162/

and reclaimed mine soil and that fertilizer treatments improved the soil quality of reclaimed mine soils (Shukla et al., 2004b). According to these studies, using several different treatments simultaneously may be better than using only one to improve the physical and chemical properties of mine soils.

In comparison with native soils, many mine soils have a higher proportion of rock fragments and possess poorer structure and coarser texture (Bussler et al., 1984). Soil texture and structure have a significant impact on water flow and contaminant transport in soils (Kodešová et al., 2009). The physical quality of coarse-textured soils (sandy, loamy sand and sandy loam) is often poor due to a high percentage of macropores, which results in losses of water and nutrients from the root zone via deep percolation and preferential flow (Asghari et al., 2011). Preferential flow may lead to rapid downward solute transport, which may cause nutrient loss and deep contamination, especially in coal mine soils, which commonly suffer from heavy metal pollution (Jiao et al., 2011; Li, 2006). Many contaminant transport solutes, including pesticides, virus, nutrition such as nitrogen and phosphorus, have been reported to bypass the soil matrix (Akhtar et al., 2011). Some researchers have studied transportation of heavy metals such as cadmium, copper, zinc, and lead in mine soils (Basta and McGowen, 2004; Runkel and Kimball, 2002). Hangen et al. (2005) assessed preferential flow processes in a forested-reclaimed lignitic mine soil by multicell sampling of drainage water and three tracers. Some non-reactive solutes, such as Br^-, Cl^- and NO_3^-, have been used as transport tracers to study solute transport processes. Valuable solute transport information can be deduced from breakthrough curves (BTCs) (Hillel, 1998), which utilize the convection dispersion equation (CDE) model.

Previous studies mostly focused on the effects of vegetation and various soil amendments on soil chemical, physical and biological properties to evaluate soil quality, in such a way, limiting factors were found in the process of vegetation restoration. A majority of studies focused on surface layers, with only a few studying deep layers. Studies on solute transport in reclaimed mine soil have not been well documented.

In this study, we focused on the physicochemical properties of soils on reclaimed waste dumps at the Heidaigou opencast coal mine, which is located on the Loess Plateau. By analyzing soil samples and conducting vertical soil column solute transport experiments, our objectives were to study the physicochemical properties and solute transport characteristics within the soil profile, to test whether the CDE model could effectively fit the solute transport parameters and to investigate the relationship between the physicochemical properties and solute transport characteristics.

2. Materials and methods

2.1. Site description

The study area is located at the Heidaigou opencast coal mine (110°13′–110°20′E, 39°43′–39°49′N), one of the largest opencast coal mines in China. The mine is located in Jungar Banner, Inner Mongolia Autonomous Region, northwest China. The area has a semi-arid, temperate continental climate, with a mean annual precipitation of 404 mm, of which approximately 64% falls between June and August (Sun et al., 2012). The average annual evaporation is approximately 2082 mm, 5 times more than the rainfall, and the mean daily temperature is 7.2 °C (Sun et al., 2012).

The Heidaigou opencast coal mine contains six waste dumps. The work of recovering the spoil banks began in 1992. The two largest waste dumps, i.e. the north waste dump, which began recovery in 1992, and the east waste dump, which began recovery in 1997. These two dumps were selected as the study area. Trees and grasses were planted to improve the soil conditions of the waste dumps, and there were no obvious dynamics in the reclaimed process. The typical vegetation types of the east waste dump were black locust (*Robinia pseudoacacia* L.) and lucerne (*Medicago sativa* L.), and those on the north waste dump were old world bluestem (*Bothriochloa ischaemum* (L.) Keng) and simon poplar (*Populus simonii Carr*). In August 2012, two plots with the corresponding typical vegetation type were selected on each of the two reclaimed waste dumps. The four sample plots were named M1, M2, M3 and M4. M1 and M2 were on the east waste dump and were dominated by black locust (*R. pseudoacacia* L.) and lucerne (*M. sativa* L.), respectively. Plots M3 and M4 were on the north waste dump and were dominated by old world bluestem (*B. ischaemum* (L.) Keng) and simon poplar (*P. simonii Carr*), respectively.

2.2. Soil sampling and analysis

The waste dumps were covered with loess soil, which was approximately 1.60–2.00 m deep. Soil samples were taken from soil profiles with a 160-cm-deep AC horizon to analyses the physical, chemical and solute transport properties (August 2012). Soil samples were collected at 20-cm intervals, and eight samples were obtained in each plot. Organic glass tubes 7.0 cm in diameter and 24 cm in height were used to collect undisturbed soil columns. The inner walls of the tubes were rubbed before the experiment to minimize the impact of the inner wall. Simultaneously, physicochemical test soil samples were obtained at 20-cm intervals and then stored in polythene bags. Once in the laboratory, the mixed samples were air-dried, screened through 2 mm, 1 mm and 0.25 mm meshes and then prepared for testing. Analyses were performed three times for each sample. The undisturbed soil columns were prepared for the solute transport experiments.

The bulk density of the soil samples was measured with stainless Kopecky cylinders. Soil cores were used to obtain the samples, and the samples were oven-dried at 105 °C for 48 h. The bulk density was calculated as the weight to volume ratio of the soil. The soil porosity was calculated with the following formula: porosity (%) = (1 − Bulk density / Particle density) × 100%.

Generally, the particle density of most soils is between 2.6 g cm^{-3} and 2.7 g cm^{-3} and is usually accepted to be 2.65 g cm^{-3}. Therefore, we used 2.65 g cm^{-3} in our calculations (Zhao et al., 2013). The distribution of soil particles was analyzed with a laser particle size analyzer (MS-2000, Malvern, Britain).

The soil pH was measured in water with a ratio of 1:2.5 using an Ion meter (Lei-ci PXSJ-216F, Shanghai REX Instrument Factory, China). Soil total nitrogen (N) was determined using an automatic Kjeldahl apparatus (2300, FOSSTECATOR, Sweden). Soil total phosphorus (P) was determined via the NaOH melting molybdenum antimony colorimetric method. Soil organic carbon (SOC) was determined using the dichromate oxidation method of Walkley–Black (Page et al., 1982). Nitrate nitrogen (NO_3^--N) and ammonium nitrogen (NH_4^+-N) were analyzed with an element flow analyzer (AutAnalyel, Bran + Luebbe GmbH, German). The cation exchange capacity (CEC) was determined after leaching 1 mm of air-dried soil with 1 M NH_4OAc at a pH of 7.0. The exchangeable cations (K^+ and Na^+) were analyzed by flame spectrophotometry (Blakemore, 1987).

A vertical soil column solute transport experiment was carried out at steady state conditions using 0.1 M NH_4NO_3 solution with specific microbial biocide as a tracer. Initially, undisturbed soil columns were placed in deionized water until the soil was completely saturated. Flow experiments were carried out by rapidly establishing and then maintaining a constant 2.0-cm head of 0.1 M NH_4NO_3 solution on the surface of the soil using a Mariotte bottle. The effluent was collected continuously in 30 ml volumetric flasks over timed intervals. The effluent samples were then analyzed using an element flow analyzer to determine the NO_3^--N and NH_4^+-N concentrations until they attained a stable level close to 0.1 M. The experiments were performed in a laboratory where the average temperature was 20 ± 3 °C. The relative humidity was not controlled but remained stable at 40 ± 10%.

2.3. Theory and model

The structural stability index (SI), a way of assessing the risk of structural degradation, was calculated using the following equation (Asensio et al., 2013; Liu et al., 2011):

$$SI = \frac{1.274 \times SOC}{silt + clay} \times 100 \quad (1)$$

where SOC is the soil organic carbon content, and (silt + clay) is the combined silt and clay content of the soil. According to Pieri (1992), a SI > 9% indicates that the structure is stable, 7% < SI ≤ 9% indicates a low risk of structural degradation, 5% < SI ≤ 7% indicates a high risk of degradation, and SI ≤ 5% indicates that the soil is structurally degraded.

The analysis of solute transport in porous media was based on the simplified convection dispersion equation (CDE) (Kasten et al., 1952; Lapidus and Amundson, 1952):

$$R\frac{\partial c}{\partial t} = D\frac{\partial^2 c}{\partial x^2} - V\frac{\partial c}{\partial x} \quad (2)$$

where R is the retardation factor, C is the concentration of solute in the liquid phase, t is the flow time, V is the pore water velocity, x is the flow distance and D is the dispersion coefficient.

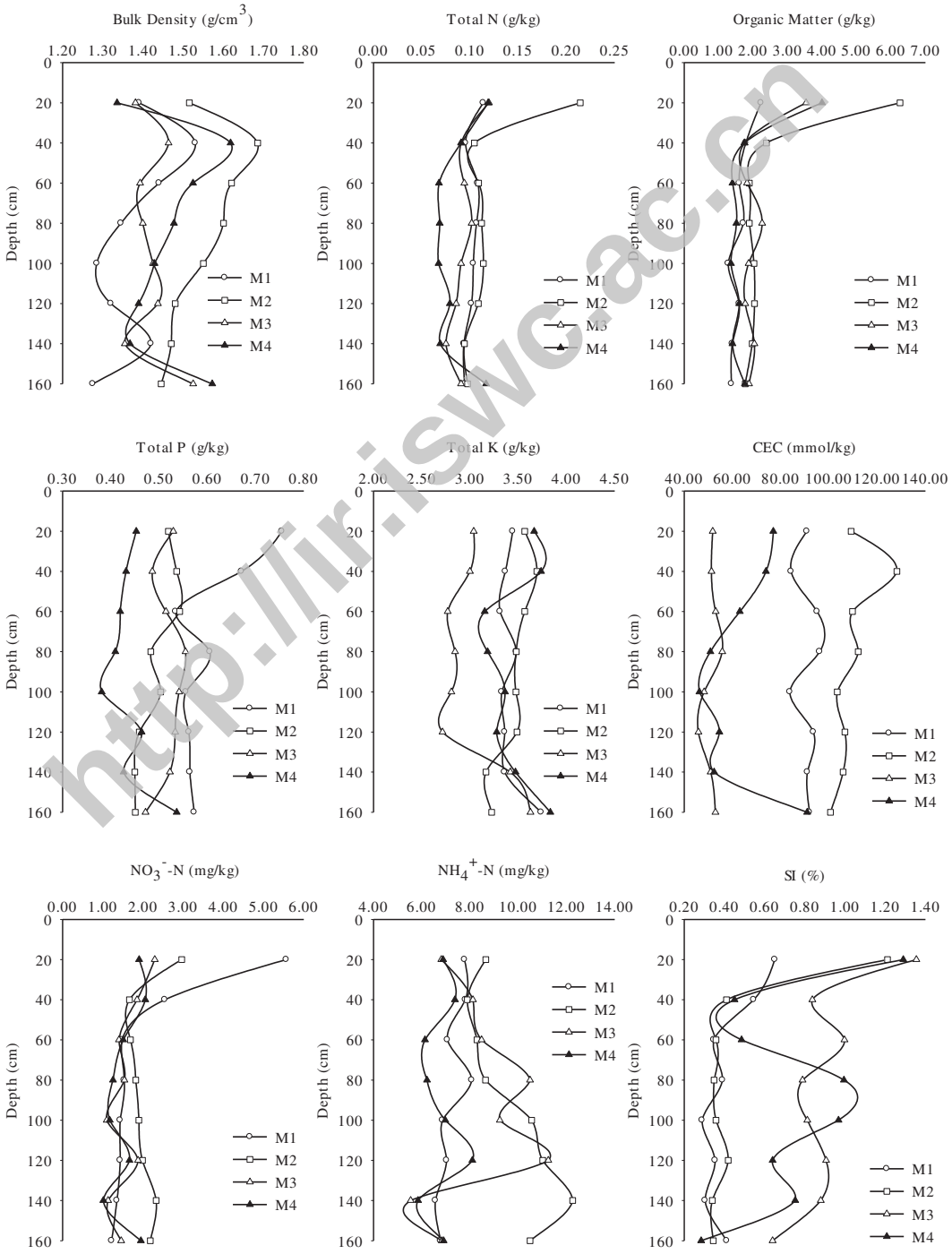

Fig. 1. Soil physicochemical properties.

Table 1
Particle size distribution.

	M1	M2	M3	M4
Sand (%)	69.93 ± 4.48a	60.15 ± 2.51b	82.53 ± 3.03c	78.44 ± 11.59c
Silt (%)	19.45 ± 3.22a	26.36 ± 1.92b	10.57 ± 2.06c	13.31 ± 7.68c
Clay (%)	10.62 ± 1.27a	13.48 ± 0.69b	6.89 ± 1.09c	8.25 ± 3.92c
Texture	Sandy loam	Sandy loam	Sandy loam	Sandy loam

Means ± SD values ($n = 8$, $P < 0.05$). Different letters indicate significant differences between the sample plots ($p < 0.05$).

The dispersivity (λ) and the Peclet number (Pe) were calculated by using the values of the dispersion coefficient derived from the CDE model, as defined by the following equations:

$$\lambda = \frac{D}{V} \tag{3}$$

$$Pe = \frac{lV}{D} = \frac{l}{\lambda} \tag{4}$$

where l is the length of the soil column.

2.4. Statistical analyses

The data were subjected to a one-way analysis of variance (ANOVA) using SPSS 17.0 for Windows (SPSS, Chicago, IL, USA). A correlated bivariate analysis was also carried out, and significant effects were reported at the 0.05 level. Additionally, regression analyses were performed, and solute transport parameters were estimated using the CXTFIT computer program (Parker and Van Genuchten, 1984; Toride et al., 1995).

3. Results and analysis

3.1. Soil physicochemical properties

The soil bulk density values ranged from 1.28 to 1.69 g cm^{-3} (Fig. 1). All 0–20 cm samples had low bulk densities, with an order of M2 > M1 > M3 > M4. The bulk densities of samples from the 20–40 cm layer were higher than those of the other layers in the soil profiles. Below 40 cm, the bulk densities decreased with increasing depth ($P < 0.05$). The 20–60 cm layer always had the most compacted soils, and other layers had looser soils.

Table 1 shows that all samples had a high proportion of sand and a low proportion of silt and clay; thus, the soil textures were characterized as sandy loam. Plot M4 had a high standard deviation and a coefficient of variation of 0.58. This reclaimed soil was coarse, and there was strong spatial variability in the soil particles.

Fig. 1 shows that the soil organic matter content decreased with increasing soil depth. The content of the surface layer (0–20 cm) was significantly higher than the deep layers ($P < 0.05$), and there were no significant differences in soil organic matter content between layers below 40 cm. The total N and NO_3^--N of the soils exhibited trends similar to the soil organic matter. Table 4 shows a significantly positive correlation between soil organic matter and total N content ($R^2 = 0.86$, $P < 0.01$). Thus, planting vegetation can improve soil organic matter and total N contents, although the contents are still considered low (Liu et al., 2011, 2013).

The trends of total P, total K, NH_4^+-N and CEC did not exhibit any notable changes related to soil depth (Fig. 1). Total P and CEC varied significantly in different sample plots. The total phosphorus levels were in the order of M1 > M3 > M2 > M4, and the CEC order was M2 > M1 > M4 > M3. There were no significant differences in total K, except for M3. The soil pH values were approximately 8.5, and there were no significant differences between plots; thus, soil pH was not shown in Fig. 1. Because NH_4^+-N primarily existed in an adsorption state, more soil adsorption sites meant higher levels of NH_4^+-N. The different soil adsorption sites of the samples and layers meant that there was no regularity in NH_4^+-N concentrations.

The SI values (Fig. 1) of all the samples were less than 5% and decreased with an increasing soil depth. The soils were therefore structurally degraded, according to Pieri (1992). The SI values in upper soil layers were significantly higher than the deeper layers ($P < 0.05$), though all samples had low SI values. A correlation analysis showed that SI and SOC were positively correlated ($R^2 = 0.58$, $P < 0.01$), and SI and silt and clay content were negatively correlated ($R^2 = 0.67$, $P < 0.01$), as shown in Table 3.

3.2. Solute transport properties

Experimental results from soil columns with different bulk densities were selected and described in Fig. 2. Smooth breakthrough curves were obtained for all columns (figure not shown). Our experimental data were fitted using the deterministic equilibrium CDE model, and

Table 2
Solute transport parameters estimated using CDE model with different samples.

Sample	V	Ts	Te	D	R	λ	Pe
	($cm \cdot h^{-1}$)	(min)	(min)	($cm^2 \cdot h^{-1}$)		(cm)	
M1	5.72 ± 0.26	148.88 ± 12.54	302.38 ± 29.09	1.34 ± 0.09	0.83 ± 0.02	0.25 ± 0.01	98.39 ± 6.58
M2	5.79 ± 0.26	170.25 ± 14.04	307.13 ± 28.85	1.16 ± 0.09	0.91 ± 0.02	0.20 ± 0.01	121.20 ± 7.26
M3	3.91 ± 0.44	223.14 ± 13.76	649.14 ± 97.60	1.35 ± 0.13	0.85 ± 0.02	0.92 ± 0.24	106.34 ± 13.32
M4	3.05 ± 0.28	383.50 ± 42.11	984.00 ± 110.43	1.45 ± 0.13	0.93 ± 0.01	0.58 ± 0.05	67.51 ± 8.95

SSQ ≤ 2.93E−02; $R^2 \geq 0.99$; MSE ≤ 2.44E−03, Ts: initial penetration time; Te: entirely penetration time; D: diffusion coefficient; R: retardation factor.

Table 3
Solute transport parameters estimated using CDE model with different layers.

Depth (cm)	V ($cm.h^{-1}$)	Ts (min)	Te (min)	D ($cm^2 \cdot h^{-1}$)	R	λ (cm)	Pe
20	5.24 ± 0.54	135.25 ± 21.08	260.75 ± 39.29	1.29 ± 0.28	0.78 ± 0.02	0.22 ± 0.03	121.42 ± 19.96
40	4.16 ± 0.52	216.50 ± 30.47	427.25 ± 59.36	1.37 ± 0.18	0.86 ± 0.04	0.36 ± 0.06	73.19 ± 8.20
60	4.53 ± 0.38	199.75 ± 32.57	372.50 ± 42.16	1.32 ± 0.28	0.87 ± 0.02	0.28 ± 0.06	137.26 ± 26.46
80	4.35 ± 0.55	277.50 ± 63.90	560.00 ± 147.22	1.26 ± 0.22	0.95 ± 0.03	0.34 ± 0.05	88.78 ± 19.94
100	4.04 ± 0.81	221.50 ± 32.55	588.00 ± 92.35	1.50 ± 0.21	0.85 ± 0.02	0.47 ± 0.09	59.72 ± 6.66
120	6.15 ± 0.87	177.25 ± 28.55	408.75 ± 112.64	1.23 ± 0.16	0.95 ± 0.04	0.39 ± 0.13	124.74 ± 19.88
140	7.40 ± 0.37	112.33 ± 4.00	210.67 ± 10.01	1.74 ± 0.33	0.99 ± 0.02	0.25 ± 0.05	100.20 ± 19.64
160	2.40 ± 0.77	554.67 ± 159.06	1343.67 ± 455.29	0.44 ± 0.04	0.84 ± 0.05	0.33 ± 0.10	105.23 ± 25.10

SSQ ≤ 2.93E−02; $R^2 \geq 0.99$; MSE ≤ 2.44E−03, Ts: initial penetration time; Te: entirely penetration time; D: diffusion coefficient; R: retardation factor.

Table 4
Correlation coefficients between soil properties and transport parameters.

	A	B	C	D	E	F	G	H	I	J	K	L	M	N	O	P	Q	R	S	T
A	1.00																			
B	0.53**	1.00																		
C	0.28	0.61**	1.00																	
D	0.16	0.42*	0.27	1.00																
E	0.29	0.26	0.04	−0.17	1.00															
F	0.85**	0.19	0.14	0.09	0.05	1.00														
G	−0.16	−0.41*	−0.26	−1.00**	0.17	−0.05	1.00													
H	0.44*	0.29	0.13	0.13	0.54**	0.37*	−0.13	1.00												
I	0.21	0.26	−0.36*	0.22	−0.01	0.10	−0.22	0.21	1.00											
J	−0.27	−0.56**	−0.12	−0.22	−0.17	−0.04	0.27	−0.23	−0.35	1.00										
K	−0.52**	−0.92**	−0.54**	−0.46**	−0.18	−0.16	0.46*	−0.21	−0.32	0.57**	1.00									
L	0.53**	0.93**	0.53**	0.45*	0.18	0.17	−0.45*	0.22	0.33	−0.59**	−1.00**	1.00								
M	0.49**	0.91**	0.57**	0.47**	0.16	0.13	−0.46*	0.20	0.28	−0.52**	−0.99**	0.99**	1.00							
N	−0.51**	−0.51**	−0.13	−0.47**	−0.24	−0.30	0.47**	−0.22	−0.33	0.35	0.54**	−0.54**	−0.55**	1.00						
O	0.20	0.42*	0.26	0.56**	0.18	0.07	−0.56**	−0.01	0.04	−0.18	−0.42*	0.42*	0.42*	−0.70**	1.00					
P	0.56**	0.58**	0.37*	0.60**	0.15	0.43*	−0.60**	0.12	0.07	−0.28	−0.54**	0.55**	0.52**	−0.74**	0.87**	1.00				
Q	0.32	0.46**	0.42*	0.06	−0.04	0.16	−0.06	0.20	0.14	−0.23	−0.43*	0.43*	0.41*	0.25	−0.41*	−0.10	1.00			
R	−0.24	−0.27	−0.14	0.32	−0.27	−0.14	−0.32	−0.32	0.04	0.28	0.26	−0.26	−0.27	0.17	0.20	0.08	−0.15	1.00		
S	0.85**	0.45*	0.29	0.29	0.03	0.77**	−0.29	0.28	0.14	−0.23	−0.41*	0.42*	0.38*	−0.42*	0.14	0.60**	0.41*	−0.18	1.00	
T	−0.52**	−0.78**	−0.59**	−0.25	−0.22	−0.23	0.25	−0.25	−0.21	0.47**	0.74**	−0.74**	−0.72**	0.34	−0.20	−0.41*	−0.67**	0.17	−0.47**	1.00

n = 31. A-T : total nitrogen; CEC; total potassium; bulk density; total phosphorus; soil organic matter; porosity; nitrate nitrogen; ammonium nitrogen; PH; sand; silt; clay; soil average pore water velocity; start penetration time; entire penetration time; D; R; λ; Pe.

* p ≤ 0.05.

** P ≤ 0.01.

the results exhibited an acceptable fitting effect. Through comparisons of the various breakthrough curves, the penetration time increases with increasing density, and penetration pore volume is increased with decreasing density. When the pore volume was equal to 1, most of the columns approached or reached full penetration.

Table 2 shows the average parameters based on the different samples. Large variations in solute transport parameters existed among the different samples, but the differences were not significant. The average pore water velocity ranged from 0.054 cm h^{-1} to 10.26 cm h^{-1}, with an order of M2 > M1 > M3 > M4. The initial penetration time and entirely penetration time ranges were 75 to 1083 min and 141 to 2884 min, respectively, with an order of M4 > M3 > M2 > M1. Table 3 shows the average parameters based on the different depths. There was an approximate trend of increased penetration time with an increasing depth, except in the 20–60 cm layer. The lowest pore water velocity, which existed at the top layer of M2, may be primarily due to compaction caused by heavy machinery. There were no significant differences in penetration time and average pore velocity between the upper soil layer and the lower layers; therefore, planting vegetation did not significantly affect the solute transport parameters.

To further study the effects of factors on the solute transport process, the BTCs were fitted well using the CDE model (SSQ ≤ 2.93E − 02; R^2 ≥ 0.99; MSE ≤ 2.44E − 03). In the CDE, the retardation factor (R) and dispersivity coefficient (D) were fitted using the BTCs. From the fitted model, the Peclet number (Pe) and the dispersivity (λ, in cm) were determined from the values obtained for D (Tables 2 and 3). There were no significant differences between the fitted parameters and the samples (Table 2). The fitted results indicated that D ranged from 0.018 to 2.82, with a mean value of 0.022 and a coefficient of variation of 0.63, representing a moderate variation. The parameter R ranged from 0.7 to 1.07, with a coefficient of variation of 0.14. The dispersivity varied from 0.077 cm to 1.174 cm, with a coefficient of variation of 1.75. The parameter Pe ranged from 4.4 to 248.15. These results indicate that the primary mode of transport was convection.

3.3. Correlation analysis of the soil properties

Table 3 shows that total N, total CEC, organic matter and soil silt and clay content were significantly positively correlated ($P < 0.01$) and also correlated with NO_3^--N ($P < 0.05$). Thus, nitrogen in the soil mostly existed in an organic state and was influenced by CEC and soil texture. Total N and sand content were significantly negatively correlated because nitrogen primarily existed as tiny particles. The CEC was significantly positively correlated with total N, total K, and silt and clay content but significantly negatively correlated with pH and sand content. Total K was significantly correlated with the CEC and silt and clay content. The soil pH and texture were also significantly correlated. In the process of mine soil reclamation, attention should be paid to improving soil texture, thereby increasing the amount of silt and clay.

The soil average pore water velocity was strongly negatively correlated with total N, CEC, bulk density, and silt and clay content ($P < 0.01$), and it was positively correlated with porosity and sand content ($P < 0.01$). The soil average pore water velocity was significantly influenced by soil quality. The soil initial penetration time and entire penetration time had similar correlations; both were positively correlated with CEC, bulk density, and silt and clay content and negatively correlated with porosity, sand content and soil average pore water velocity. The two times differed in that the entire soil penetration time also had a positive correlation with total N ($P < 0.01$), total K and organic matter ($P < 0.05$).

4. Discussion

4.1. Soil physicochemical properties

The soil bulk densities ranged from 1.28 to 1.69 g cm^{-3}, with an average of 1.45 g cm^{-3}. The undisturbed original soil had a bulk density

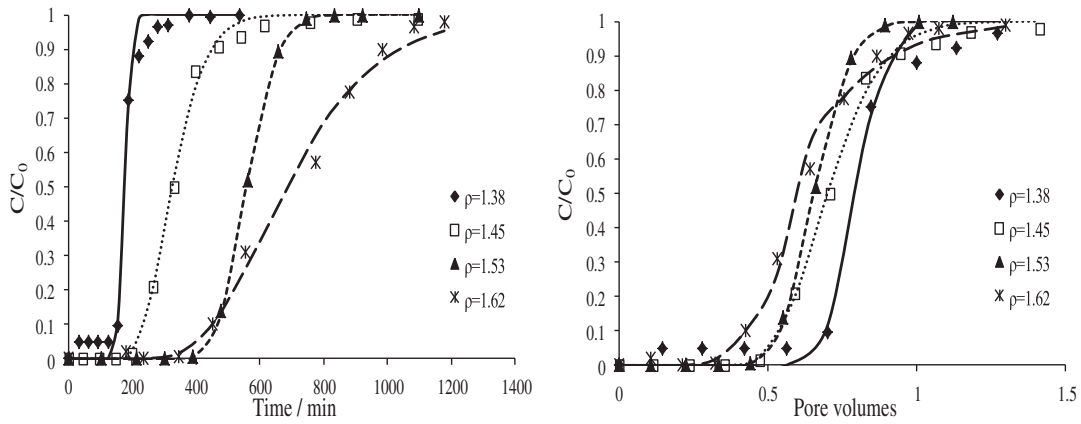

Fig. 2. BTCs for soil experiment and fitting with different bulk densities (point is test value and line is fitted value by CDE model).

of less than 1.40 g cm^{-3} on the Loess Plateau (Jiao et al., 2011). The waste dumps have been compressed by large machinery, leading to high levels of compaction and high bulk densities, especially in the surface layer. The layers at 20–60 cm had the most compacted soils, and the deeper layers had looser soils. The decrease in bulk density in the upper soils could be due to root penetration, soil breakdown and an increase in the number of pores (Asensio et al., 2013). The variations between different soil profiles may be due to differences in soil texture. Although all the soils were sandy loam, significant differences were present in the sand, silt and clay contents.

In general, the nitrogen and organic matter contents of mine soils are low, which limits vegetation establishment and sustainable productivity (Li, 2006; Zhao et al., 2013). In most natural ecosystems, N inputs are minimal, and N retention and efficient cycling are critical for maintenance of ecosystem productivity (Mummey et al., 2002). In our study, the values of total N are nearly less than 0.2 g kg^{-1}. Compared with other studies (Keskin and Makineci, 2009; Wong and Ho, 1993), the N content is very low; hence, the accumulation of even small amounts of nitrogen in mine soil/spoil is very important (Sever and Makineci, 2009). There was a marked increase in both organic matter and total

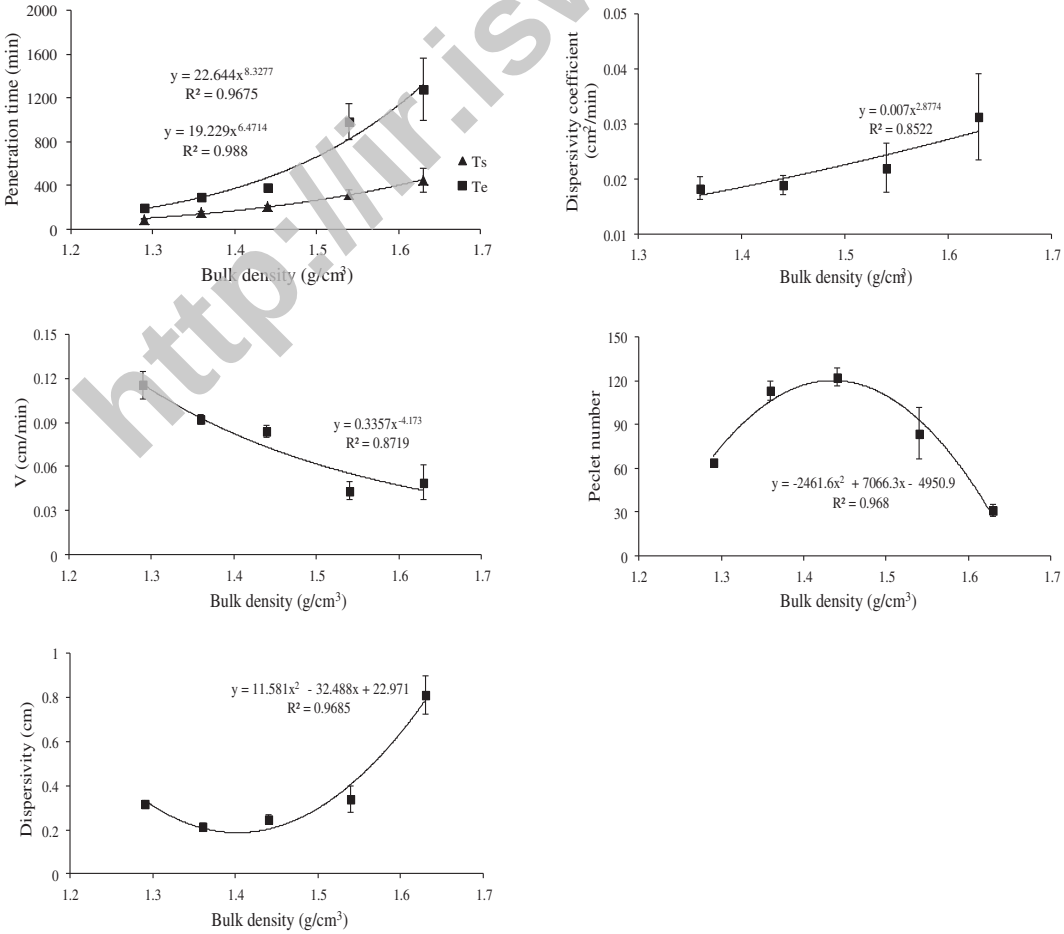

Fig. 3. Relations between solute transport parameters and bulk density.

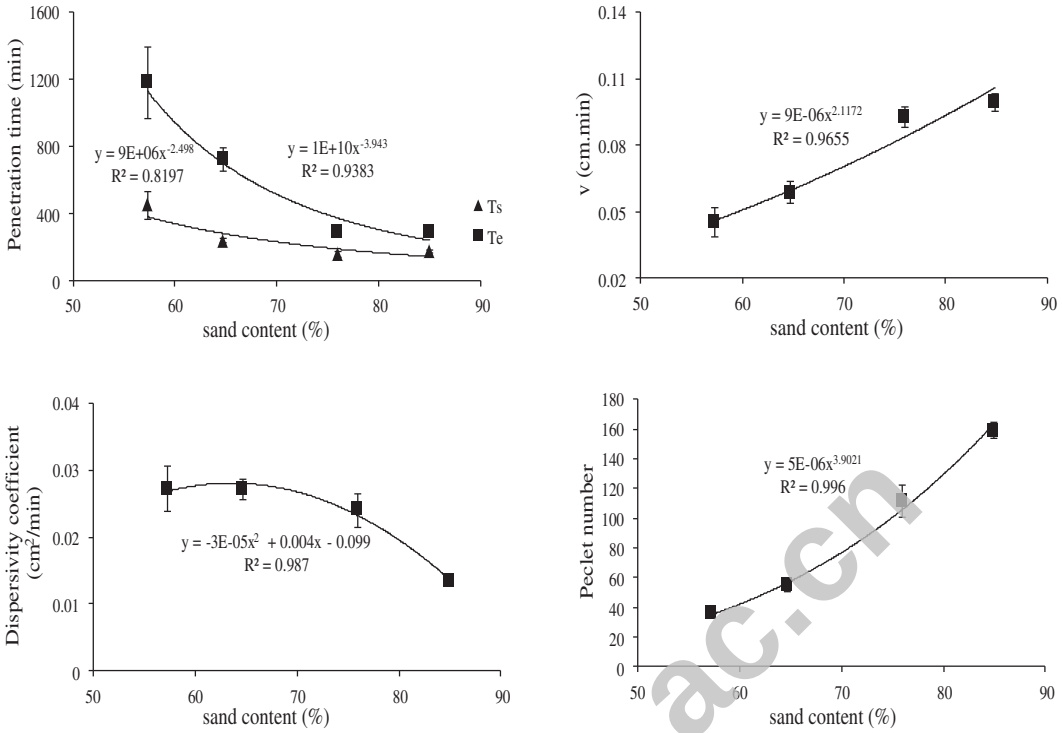

Fig. 4. Relations between solute transport parameters and sand cont.

N levels in the 0–20 cm layers in the spoil. This could be attributed to planting vegetation, which improved the organic matter and total N contents (Asensio et al., 2013). The total N content was influenced by soil texture; the correlation matrix showed that there was a significant correlation between total N and distribution of soil particles. More work should be performed to study whether plant species and reclamation time have any effect on total N content because the 0–20 cm layer of M2 had higher total N levels than the other plots.

Soil nitrate is a type of water-soluble nitrogen, which generally exists in the soil solution in the free state (Stevenson and Cole, 1999). In the soil, NH_4^+-N primarily exists in an adsorption state. Thus, more soil adsorption sites results in higher levels of NH_4^+-N. The irregular trend of NH_4^+-N was a result of the different soil adsorption sites between each sample and various layers. As shown in the correlation matrix, NO_3^--N and NH_4^+-N do not exhibit a significant correlation with total N and organic matter, which is in agreement with the results of Mummey et al. (2002). The inorganic N concentrations vary spatially and have a lack of significant correlation with SOM, suggesting that the N cycle of this system is less efficient or less tightly coupled than in an undisturbed ecosystem (DeLuca and Keeney, 1993; Smith, 1994).

The formation and accumulation of organic matter are the major processes that determine the direction and speed of initial pedogenesis (Evgeny and Jan, 2013; Filcheva et al., 2000). In mining soil, the accumulation of organic matter and organic carbon has been previously considered to be the key factor for the activation of biological soil processes (Fu et al., 2010; Lorenz and Lal, 2007). In our study, the organic content of the surface layer is significantly higher than the deeper layers, indicating that planting vegetation improves the physical soil structure of the degraded land.

The content of total P is mainly determined by the parent material types and the application of phosphate fertilizer. These factors could explain the variation in the total P content. The total K values did not present any notable trends related to soil depth, and total K was primarily influenced by soil texture, as demonstrated by the correlation matrix, which showed that total potassium was significantly correlated with CEC and soil texture. The CEC varied between different plots, but there were no depth-related variations, except for M4. The CEC was significantly correlated with the silt and clay content of the soils ($R^2 > 0.91$, $P < 0.01$), and the distribution of soil particles at M4 had a high standard deviation and a coefficient of variation of 0.58, which may explain the CEC fluctuations at M4.

4.2. Soil solute transport parameters

Previous studies used a pore volume of $V/V_0 < 1$ when the relative concentrations of the undisturbed soil column were $C/C_0 = 0.5$ as evidence of the existence of preferential flow (Singh and Kanwar, 1991). If no preferred path exists, then when the pore volume value equals 1, the outflow level is equal to the moisture content of the saturated soil column. In other words, the volume of moisture in the soil column is equal to the volume of the input solution. Therefore, the solution concentration is diluted to just 50% of the original solution concentration, and the relative concentration is equal to 0.5. Experimental results showed that when C/C_0 was equal to 0.5, V/V_0 was almost less than 1. In our study, preferential flow existed in the solute transport in the undisturbed soil columns at the opencast coal mine site. Although scholars have given different definitions of preferential flow (Beven and Germann, 1982; Luxmoore et al., 1990; White, 1985), the existence of preferential flow unquestionably leads to rapid solute transport, which may cause deep pollution (Jarvis, 2007). In the study area, vegetation and the changes in soil texture and structure were the main factors influencing the formation of preferential soil pathways. Although the samples exhibited high heterogeneity in penetration time, the initial and entire penetration times were both significantly influenced by CEC, bulk density, soil texture and average soil pore water velocity. Moreover, the entire penetration time was significantly correlated with total N and organic matter. Soils with a fine texture appeared to have a longer penetration time than soils with a coarse texture. According to the study of Parker and Van Genuchten (1984), the typical characteristic of non-reactive solute was $R \approx 1$, and the typical characteristic of reactive solute was $R > 1$. In the study, NO_3^- was a non-reactive solute, so $R \leq 1$ (Zhou et al. (2013)).

4.3. Effect of bulk density on solute transport parameters

The regression analyses, performed for all data, evaluated the relationships between the soil bulk density and solute transport parameters. In this study, the relationship between the average soil pore water velocity, penetration time, D and bulk density could be modeled as a power law (Fig. 3). Among them, v decreased with increasing ρ, indicating a negative power function relationship. Penetration time and D increased with increasing bulk density, which is in agreement with the results of Lv et al. (2010). This relationship exists because an increase in bulk density represents a more compacted soil and a lower pore volume. As a result, the pore space of water movement is reduced, and the decreased flow rate results in reduced convective solute transport and enhanced dispersion effects.

Dispersivity is an experimental parameter, and its value in coarse-textured and homogeneous soils is often less than in fine-textured and heterogeneous soils (Perfect et al., 2002; Vanderborght and Vereecken, 2007). The dispersivity parameter assumes a quadratic function relationship between λ and ρ. When ρ is close to 1.4 g cm^{-3}, the λ value approaches its lowest value. Previous laboratory test results have shown that λ ranges from 0.20 to 0.55 cm (Bejat et al., 2000). In this study, the mean value of λ was 0.33 cm. When the average ρ was 1.63 g cm^{-3}, λ is 0.812 cm. The result can be attributed to the larger ρ and the smaller v. Pe is a dimensionless number, used to represent the convection and diffusion ratio. As the value of Pe increases, the convective transport ratio also increases, but the diffusion transport ratio decreases. In this study, the values of Pe were far greater than 1, indicating that convection was the primary mode of solute transport.

4.4. Effect of particles on solute transport parameters

In this study, the relationship between average soil pore water velocity, penetration time, Peclet number and sand content could be modeled as a power law (Fig. 4). Among them, penetration time decreased with increasing sand content, showing a negative power function relationship. Pe and v increased with increasing sand content. D decreased with increasing sand content when the value was larger than 60%. Clearly, soil texture is one of the most important factors affecting solute transport. The soil porosity, water holding capacity and physical–mechanical properties featured significant differences due to the differences in the soil textures. In the fine-textured soils, with more clay and less sand, the transport ions are strongly adsorbed by the clay, which possesses a much larger specific surface area than sand. As clay content increases, the capillary action caused by the soil pore radius is reduced. As a result, the average velocity of solution transport in capillaries is reduced. Therefore, the transported ions do not easily penetrate the soil (Shang et al., 2008).

5. Conclusions

This study described the results from 4 plots, with 160-cm soil profiles and different vegetation, on reclaimed opencast coal mine waste dumps on the Loess Plateau in northwest China. The land was severely structurally degraded, and the addition of vegetation was shown to improve the soil properties. In areas with vegetation, the surface layer had a lower bulk density and higher contents of total nitrogen and soil organic matter compared with the deeper layers. The vertical undisturbed soil column solute transport experiment showed that preferential flow was ubiquitous in the reclaimed soils. The CDE equation model fitted the solute transport processes well. The experimental data and fitted parameters indicated that increased bulk density and increased silt and clay content could reduce the average soil pore water velocity and dispersivity coefficient, thus extending the solute penetration time. Due to the effect of plant roots, the penetration time for the topsoil was shorter. Therefore, during the process of soil remediation, fine textures and appropriate densities should be given more consideration, and planting vegetation is a useful way to improve the properties of reclaimed soil.

Acknowledgments

We thank Yan-jiang Zhang for his help with the field and laboratory experiments. We are grateful to Ji-yong Zheng for help operating the CXTFIT program. This study was supported by the Program funded by the Chinese Academy of Sciences (KZCX2-XB3-13-02), the National Natural Science Foundation of China (41101528, 41471437) and the West Light Foundation of Chinese Academy of Sciences to Yi Wang.

References

Akhtar, M.S., Stüben, D., Norra, S., Memon, M., 2011. Soil structure and flow rate-controlled molybdate, arsenate and chromium(III) transport through field columns. Geoderma 161, 126–137.
Asensio, V., Vega, F.A., Andrade, M.L., Covelo, E.F., 2013. Tree vegetation and waste amendments to improve the physical condition of copper mine soils. Chemosphere 90, 603–610.
Asghari, S., Abbasi, F., Neyshabouri, M.R., 2011. Effects of soil conditioners on physical quality and bromide transport properties in a sandy loam soil. Biosyst. Eng. 109, 90–97.
Basta, N.T., McGowen, S.L., 2004. Evaluation of chemical immobilization treatments for reducing heavy metal transport in a smelter-contaminated soil. Environ. Pollut. 127, 73–82.
Bejat, L., Perfect, E., Quisenberry, V., Coyne, M.S., Haszler, G., 2000. Solute transport as related to soil structure in unsaturated intact soil blocks. Soil Sci. Soc. Am. J. 64, 818–826.
Beven, K., Germann, P., 1982. Macropores and water flow in soils. Water Resour. Res. 18, 1311–1325.
Blakemore, L.C., 1987. Extractable iron, aluminium and silicon. In methods for chemical analysis of soils. N. Z. Soil Bur. Sci. Rep. 80, 71–76.
Bussler, B., Byrnes, W., Pope, P., Chaney, W., 1984. Properties of minesoil reclaimed for forest land use. Soil Sci. Soc. Am. J. 48, 178–184.
Carter, M.R., et al., 1997. Concepts of Soil Quality and Their Significance. Developments in Soil Science. Elsevier Science Publisher, Amsterdam, pp. 1–19.
DeLuca, T., Keeney, D., 1993. Soluble organics and extractable nitrogen in paired prairie and cultivated soils of central Iowa. Soil Sci. 155, 219–228.
Evgeny, A., Jan, F., 2013. Humus Accumulation and Humification During Soil Development in Post-mining Soil, Soil Biota and Ecosystem Development in Post Mining Sites. CRC Press, pp. 19–37.
Filcheva, E., Noustorova, M., Gentcheva-Kostadinova, S., Haigh, M.J., 2000. Organic accumulation and microbial action in surface coal-mine spoils, Pernik, Bulgaria. Ecol. Eng. 15, 1–15.
Fu, Y., Lin, C., Ma, J., Zhu, T., 2010. Effects of plant types on physico-chemical properties of reclaimed mining soil in Inner Mongolia, China. Chin. Geogr. Sci. 20, 309–317.
Hangen, E., Gerke, H.H., Schaaf, W., Hüttl, R.F., 2005. Assessment of preferential flow processes in a forest-reclaimed lignitic mine soil by multicell sampling of drainage water and three tracers. J. Hydrol. 303, 16–37.
Hillel, D., 1998. Environmental soil physics: fundamentals, applications, and environmental considerations. Academic press, San Diego.
Jarvis, N., 2007. A review of non-equilibrium water flow and solute transport in soil macropores: principles, controlling factors and consequences for water quality. Eur. J. Soil Sci. 58, 523–546.
Jiao, F., Wen, Z.M., An, S.S., 2011. Changes in soil properties across a chronosequence of vegetation restoration on the Loess Plateau of China. Catena 86, 110–116.
Kasten, P.R., Lapidus, L., Amundson, N.R., 1952. Mathematics of adsorption in beds. V. Effect of intra-particle diffusion in flow systems in fixed beds. J. Phys. Chem. 56, 683–688.
Keskin, T., Makineci, E., 2009. Some soil properties on coal mine spoils reclaimed with black locust (*Robinia pceudoacacia* L.) and umbrella pine (*Pinus pinea* L.) in Agacli-Istanbul. Environ. Monit. Assess. 159, 407–414.
Kodešová, R., et al., 2009. Impact of varying soil structure on transport processes in different diagnostic horizons of three soil types. J. Contam. Hydrol. 104, 107–125.
Lapidus, L., Amundson, N.R., 1952. Mathematics of adsorption in beds. VI. The effect of longitudinal diffusion in ion exchange and chromatographic columns. J. Phys. Chem. 56, 984–988.
Li, M.S., 2006. Ecological restoration of mineland with particular reference to the metalliferous mine wasteland in China: a review of research and practice. Sci. Total Environ. 357, 38–53.
Liu, Z., Shao, M.A., Wang, Y., 2011. Effect of environmental factors on regional soil organic carbon stocks across the Loess Plateau region, China. Agric. Ecosyst. Environ. 142, 184–194.
Liu, Z.P., Shao, M.A., Wang, Y.Q., 2013. Spatial patterns of soil total nitrogen and soil total phosphorus across the entire Loess Plateau region of China. Geoderma 197–198, 67–78.
Lorenz, K., Lal, R., 2007. Stabilization of organic carbon in chemically separated pools in reclaimed coal mine soils in Ohio. Geoderma 141, 294–301.
Luxmoore, R., Jardine, P., Wilson, G., Jones, J., Zelazny, L., 1990. Physical and chemical controls of preferred path flow through a forested hillslope. Geoderma 46, 139–154.

Lv, D.Q., Wang, H., Pan, Y., Wang, L., 2010. Effect of bulk density changes on soil solute transport characteristics. J. Nat. Sci. Hunan Norm. Univ. 33, 75–79 (in Chinese).
Mummey, D.L., Stahl, P.D., Buyer, J.S., 2002. Soil microbiological properties 20 years after surface mine reclamation: spatial analysis of reclaimed and undisturbed sites. Soil Biol. Biochem. 34, 1717–1725.
Page, A., Miller, R., Keeney, D., 1982. Total carbon, organic carbon, and organic matter. Methods of soil analysis. Part 2, Chemical and microbiological propertiespp. 539–579.
Palumbo, A., et al., 2004. Prospects for enhancing carbon sequestration and reclamation of degraded lands with fossil-fuel combustion by-products. Adv. Environ. Res. 8, 425–438.
Parker, J., Van Genuchten, M.T., 1984. Determining transport parameters from laboratory and field tracer experiments. Virginia Agric. Exp. Stat., Bull. Blacksburg p. 84-3.
Pedrol, N., et al., 2010. Soil fertility and spontaneous revegetation in lignite spoil banks under different amendments. Soil Tillage Res. 110, 134–142.
Perfect, E., Sukop, M., Haszler, G., 2002. Prediction of dispersivity for undisturbed soil columns from water retention parameters. Soil Sci. Soc. Am. J. 66, 696–701.
Pieri, C.J., 1992. Fertility of soils: a future for farming in the West African savannah. Springer-Verlag, Berlin.
Runkel, R.L., Kimball, B.A., 2002. Evaluating remedial alternatives for an acid mine drainage stream: application of a reactive transport model. Environ. Sci. Technol. 36, 1093–1101.
Sever, H., Makineci, E., 2009. Soil organic carbon and nitrogen accumulation on coal mine spoils reclaimed with maritime pine (Pinus pinaster Aiton) in Agacli-Istanbul. Environ. Monit. Assess. 155, 273–280.
Shang, J., Flury, M., Chen, G., Zhuang, J., 2008. Impact of flow rate, water content, and capillary forces on in situ colloid mobilization during infiltration in unsaturated sediments. Water Resour. Res. 44, 6.
Shrestha, R.K., Lal, R., 2006. Ecosystem carbon budgeting and soil carbon sequestration in reclaimed mine soil. Environ. Int. 32, 781–796.
Shukla, M., Lal, R., Ebinger, M., 2004a. Soil quality indicators for reclaimed minesoils in southeastern Ohio. Soil Sci. 169, 133–142.
Shukla, M., Lal, R., Underwood, J., Ebinger, M., 2004b. Physical and hydrological characteristics of reclaimed minesoils in southeastern Ohio. Soil Sci. Soc. Am. J. 68, 1352–1359.
Singh, P., Kanwar, R.S., 1991. Preferential solute transport through macropores in large undisturbed saturated soil columns. J. Environ. Qual. 20, 295–300.
Smith, J., 1994. Cycling of nitrogen through microbial activity. Soil biology: effects on soil quality. Lewis Publishers, Boca Raton.
Stevenson, F.J., Cole, M.A., 1999. Cycles of Soils: Carbon, Nitrogen, Phosphorus, Sulfur, Micronutrients. John Wiley & Sons, New York.
Sun, T.S., Li, B., Zhang, X.S., 2012. The response of agro-ecosystem productivity to climatic fluctuations in the farming-pastoral ecotone of northern China: a case study in Zhunger County. Acta Ecol. Sin. 32, 6155–6167 (in Chinese).
Toride, N., Leij, F., Van Genuchten, M.T., 1995. The CXTFIT code for estimating transport parameters from laboratory or field tracer experiments. Research Report No. 137 US Salinity Laboratory, US Department of Agriculture, Riverside, CA.
Vanderborght, J., Vereecken, H., 2007. Review of dispersivities for transport modeling in soils. Vadose Zone J. 6, 29–52.
Wang, Y.H., Guo, D.Z., Zang, H.R., Shen, B.G., 2006. Spatial distribution and application of coal resource potential in China. J. Nat. Resour. 21, 225–230 (in Chinese).
White, R., 1985. The transport of chloride and non-diffusible solutes through soil. Irrig. Sci. 6, 3–10.
Wong, M., 2003. Ecological restoration of mine degraded soils, with emphasis on metal contaminated soils. Chemosphere 50, 775–780.
Wong, J.W.C., Ho, G.E., 1993. Use of waste gypsum in the revegetation on red mud deposits: a greenhouse study. Waste Manag. Res. 11, 249–256.
Zhao, Z., et al., 2013. Soils development in opencast coal mine spoils reclaimed for 1–13 years in the West-Northern Loess Plateau of China. Eur. J. Soil Biol. 55, 40–46.
Zhou, B.B., Li, Y., Wang, C.L., Jiang, Y.L., Li, S., 2013. Preferential water and solute transport through sandy soil containing artificial macropores. Environ. Earth Sci. 70, 2371–2379.